PACS numbers: 71.15.Mb, 78.30.-j, 78.40.-q, 78.67.Bf, 81.05.Zx, 85.60.Bt, 87.85.Qr

# Analysis and Characteristics of Nanostructures for Biomedical Applications

Hussein Hakim Abed[1], Ahmed Hashim[2], Mudar Ahmed Abdulsattar[3], and Hayder M. Abduljalil[4]

[1]*Department of Physics,*
*College of Science,*
*University of Babylon, Iraq*
[2]*Department of Physics,*
*College of Education of Pure Science,*
*Babylon University, Iraq*
[3]*Department of Physics,*
*College of Science,*
*University of Babylon, Iraq*
[4]*Ministry of Science and Technology,*
*Baghdad, Iraq*

The cubic structures of zinc sulphide and ternary alloys from zinc, cadmium, and sulphide atoms at the nanoscale regime have been represented by nanostructures called tetramantane ($Zn_{11}S_{11}$, $Zn_{11-n}Cd_nS_{11}$ ($n = 1$, ..., 3)). The electronic properties: HOMO, LUMO, and HOMO−LUMO gap have been investigated. They were found as affected by cadmium concentrations and converge to practical results. Infrared and Raman spectra of ternary alloys referred to occur with shifting in maximum peak and appearing a new peak different from infrared and Raman spectra of nanostructure for zinc sulphide due to connecting between zinc, cadmium, and sulphide atoms. UV−Vis spectra for nanostructures have been examined; the maximum peak and the optical-edge absorption are shifted to lower energy. In addition, the width of peaks increase with increased quantity of cadmium atoms. From results, these nanostructures are suitable to be used in optoelectronics and biosensors for biomedical applications. Density functional theory and time-dependent density functional theory at the B3LYP level with SDD-basis functions are used. All the results are obtained by using the Gaussian 09 program.

Кубічні структури сульфіду Цинку та тернарних стопів з атомів Цинку, Кадмію та сульфіду на наномасштабному режимі були представлені наноструктурами, званими тетрамантаном ($Zn_{11}S_{11}$, $Zn_{11-n}Cd_nS_{11}$ ($n = 1$, ..., 3)). Досліджено електронні властивості: HOMO, LUMO та HOMO−

LUMO щілину. Вони були виявлені як порушені концентрацією Кадмію і зосереджуються на практичних результатах. Інфрачервоні та Раманові спектри тернарних стопів, про які йдеться, відбуваються зі зміщенням у максимальному піку та появою нового піку, відмінного від інфрачервоних і Раманових спектрів наноструктури для сульфіду Цинку через з'єднання між атомами Цинку, Кадмію та сульфіду. Досліджено спектри у видимій і ультрафіолетовій областях світла для наноструктур; максимальний пік і край оптичного поглинання зміщуються до більш низької енергії. Крім того, ширина піків збільшується зі збільшенням кількости атомів Кадмію. За результатами ці наноструктури підходять для використання в оптоелектроніці та біосенсорах для біомедичних застосувань. Використовується теорія функціоналу густини та теорія функціоналу густини, що залежить від часу, на рівні гібридного B3LYP-функціоналу з набором SDD-базисних функцій. Всі результати одержано за допомогою програми Ґауссіян 09.

## 1. INTRODUCTION

Nanostructures have quantum confinement effect and size-dependent properties; therefore, the electrical, optical, thermoelectric and magnetic properties of materials modify by using nanostructures [1]. The II–VI nanostructures signify interesting attention of experimental and computational study, which can be used in wide applications in different fields such as industrial and biomedical. Nanostructures represent the bridge between molecular and bulk material. Some nanostructures exhibit remarkable stability than others maybe because of geometric configurations or electronic state [2]. Zinc sulphide and cadmium sulphide crystallize in two forms cubic (zinc blende) and hexagonal (wurtzite) at room temperature, ZnS and CdS have high band gaps and important materials in many applications such as solar energy conversion, optical mass memories, infrared windows, light-emitting diodes (LEDs), nonlinear optical devices, sensors, lasers, and photocatalysis due to its varied range of promising structures and morphologies, stability and their potential application in a new generation of optoelectronics devises [3, 4]. The formation of ternary alloys $Zn_{11-n}Cd_nS_{11}$, of varying concentrations of zinc and cadmium atoms, offers the possibility of obtaining a material having the ability to regulate physical properties. Ternary alloys from Zn, Cd, and S atoms are reflected as a favourable material in the construction of photodetector, biomedi-

cal labels, solar cells, and optically controlled switches [5].

The cubic structure of ZnS at the nanoscale regime was represented by $Zn_{11}S_{11}$ nanostructures. To get ternary alloy $Zn_{11-n}Cd_nS_{11}$, zinc atoms were replaced by cadmium atoms for ($n = 1-3$). This work aims to investigate the HOMO and LUMO levels, IR spectra, Raman spectra, and UV–Vis spectra for these nanostructures by using the Gaussian 09 program, density functional theory, and time-dependent density functional theory at the B3LYP level with SDD-basis function.

## 2. METHODS

Cubic (zinc blende) and hexagonal (wurtzite) structures at the nanoscale regime can be represented by nanostructures called diamondoids and wurtzoids, respectively [6–10]. Clusters and nanostructures from ZnS, ZnSe, CdS, and CdSe have been reported previously by others [11]. In the present work, ZnS cubic diamondoid was used to represent ZnS nanocrystals. Tetramantane $Zn_{11}S_{11}$ was used as a representative of this diamondoid due to its appropriate base size and gave results converged to experimental measurements. Figure 1 shows tetramantane $Zn_{11}S_{11}$ after geometric optimization.

Ternary alloys of Zn, Cd and S atoms with compositions $Zn_{11-n}Cd_nS_{11}$ ($n = 1-3$) including $Zn_{10}CdS_{11}$, $Zn_9Cd_2S_{11}$, and $Zn_8Cd_3S_{11}$ are shown in Fig. 1 after geometric optimization. After getting the preferred configurations by optimized nanostructures, the IR spec-
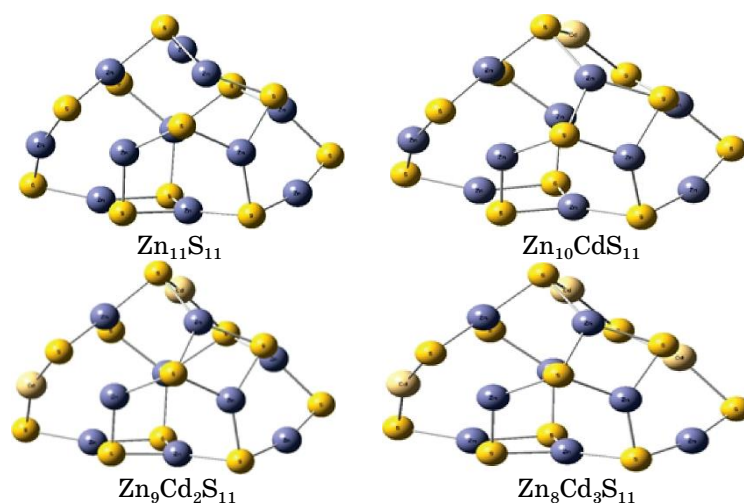


**Fig. 1.** Tetramantane $Zn_{11}S_{11}$ and ternary alloys of $Zn_{11}CdS_{10}$, $Zn_{11}Cd_2S_9$, and $Zn_{11}Cd_3S_8$ after optimization.

tra, Raman spectra, and UV−Vis spectra investigated and compared with experimental measurements. All calculations have been performed by using DFT/TDDFT at the B3LYP level with the SDD-basis function by Gaussian 09 program [12].

## 3. RESULTS AND DISCUSSIONS

### 3.1. Energy Gap

Nanostructures have size and shape-dependent properties. In this work, $Zn_{11}S_{11}$ and ternary alloys $Zn_{11-n}Cd_nS_{11}$ have a size of a few nanometres; therefore, confinement effect is prevailing and leads to change in the density of the states and separation in the energy levels [1, 13]. The relation between the energy gap, HOMO, and LUMO levels as a function of increasing the number of cadmium atoms are shown in Fig. 2. $Zn_{11}S_{11}$ has energy gap of 3.597374 eV in high agreement with experimental value of 3.6 eV [14]. When the concentrations of cadmium atoms increased, the HOMO levels increased, and the LUMO levels decreased, as shown in Fig. 2. Therefore, the LUMO−HOMO gap condensed and become of 3.088244 eV for $Zn_8Cd_3S_{11}$, as shown in Table 1. From Figure 3, the high occu-
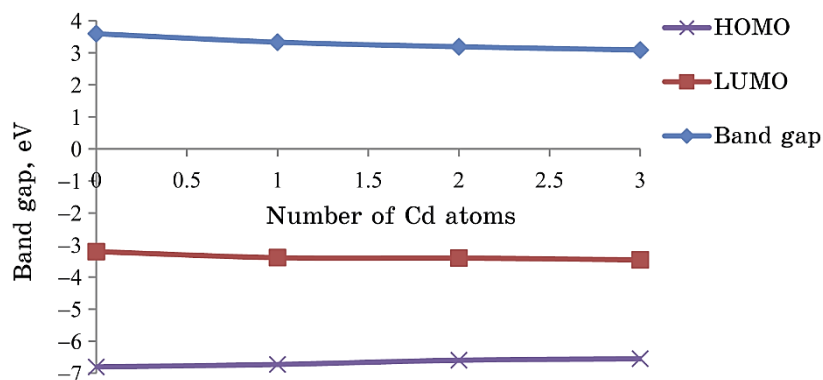


**Fig. 2.** Variations of the energy gap with Cd atom.

**TABLE 1.** The HOMO and LUMO levels and bandgap.

| Nanostructures | HOMO, eV | LUMO, eV | Bandgap, eV |
|---|---|---|---|
| $Zn_{11}S_{11}$ | −6.8029 | −3.20553 | 3.597374 |
| $Zn_{10}CdS_{11}$ | −6.72698 | −3.39356 | 3.333421 |
| $Zn_9Cd_2S_{11}$ | −6.59528 | −3.40526 | 3.190016 |
| $Zn_8Cd_3S_{11}$ | −6.54874 | −3.4605 | 3.088244 |

HOMOZn$_{11}$S$_{11}$                    LUMOZn$_{11}$S$_{11}$

HOMO-Zn$_{10}$CdS$_{11}$                  LUMO-Zn$_{10}$CdS$_{11}$

HOMOZn$_9$Cd$_2$S$_{11}$                  LUMOZn$_9$Cd$_2$S$_{11}$

HOMO-Zn$_8$Cd$_3$S$_{11}$                 LUMO-Zn$_8$Cd$_3$S$_{11}$
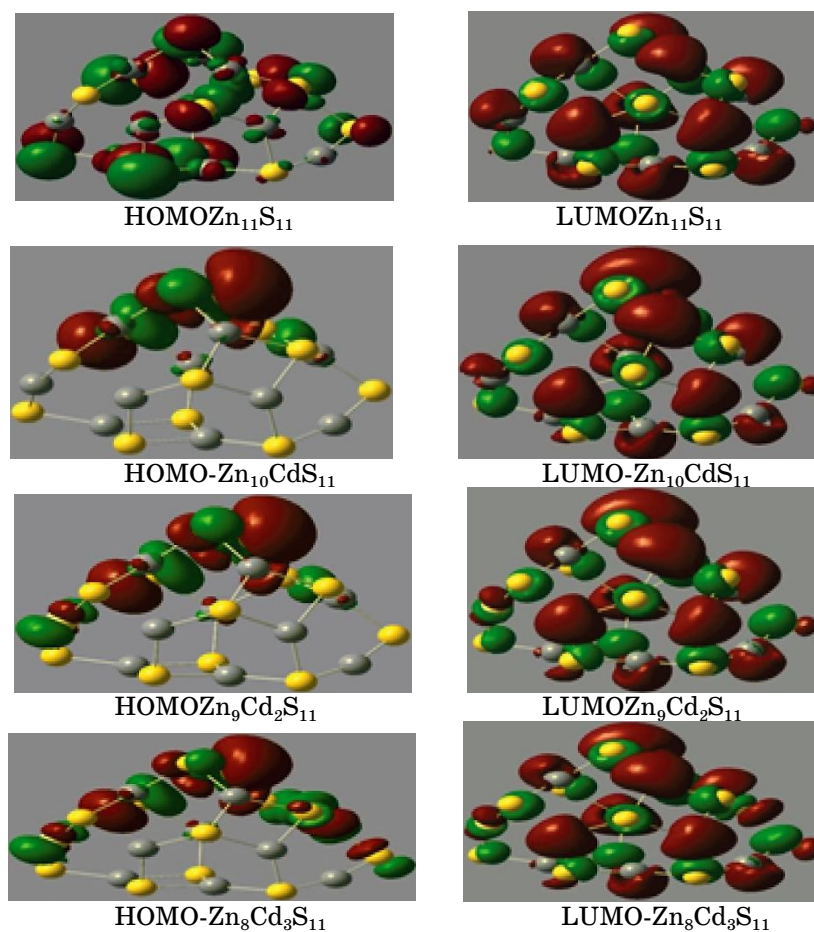
**Fig. 3.** HOMO and LUMO levels for nanostructures.

pied molecular orbital (HOMO) is affected and concerned by cadmium atoms. The capability to control the value of the energy gap by changing the composition of ternary alloys is performed in different applications such as optoelectronic devices and biosensors [15].

### 3.2. IR Spectra

Figure 4 shows the IR spectra for ternary alloys nanostructures. $Zn_{11}S_{11}$ has maximum peaks at 346 cm$^{-1}$ corresponding to zinc and sulphide stretching, its agreement with experimental [16]. After replaced zinc atoms by cadmium atoms, clear appear new peak for IR spectrum at 382.3 cm$^{-1}$ of $Zn_9Cd_2S_{11}$ and 381.2 cm$^{-1}$ of $Zn_8Cd_3S_{11}$ because of presenting vibrations from Cd–S–Zn bonds, which in-
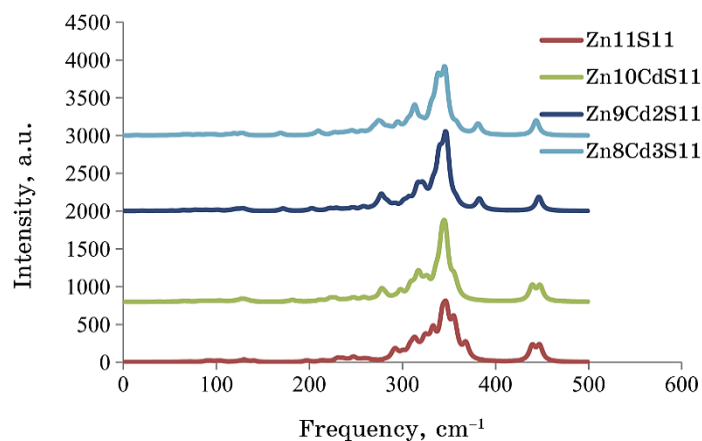
**Fig. 4.** IR spectra for nanostructures.
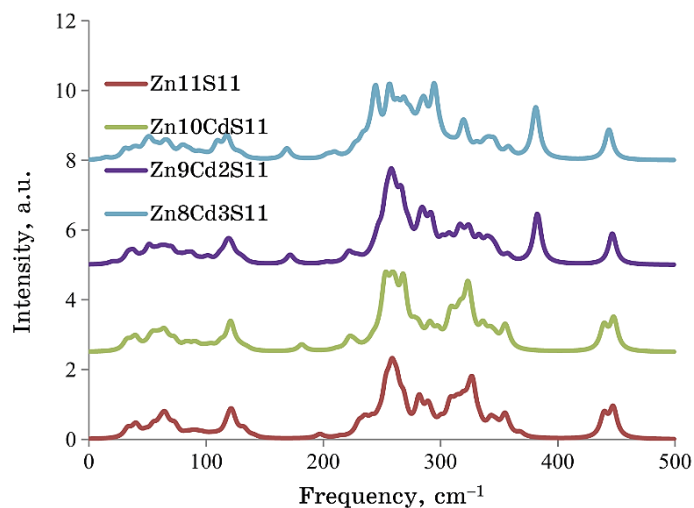


**Fig. 5.** Raman spectra for ternary-alloys' nanostructures.

creased with increased cadmium atoms.

## 3.3. Raman Spectra

The composition and symmetry of nanostructures are the main factors to constitute the Raman spectra for ternary alloys, as shown in Fig. 5.

Raman shift changed with compositions [17]. $Zn_{11}S_{11}$ has a maximum peak at frequency 256 cm$^{-1}$, which moves left to the experi-

**TABLE 2.** Maximum peaks for the Raman spectrum.

| Nanostructures | Maximum peak, $cm^{-1}$ |
|---|---|
| $Zn_{11}S_{11}$ | 256 |
| $Zn_{10}CdS_{11}$ | 253 |
| $Zn_9Cd_2S_{11}$ | 255.8 |
| $Zn_8Cd_3S_{11}$ | 243.7 |
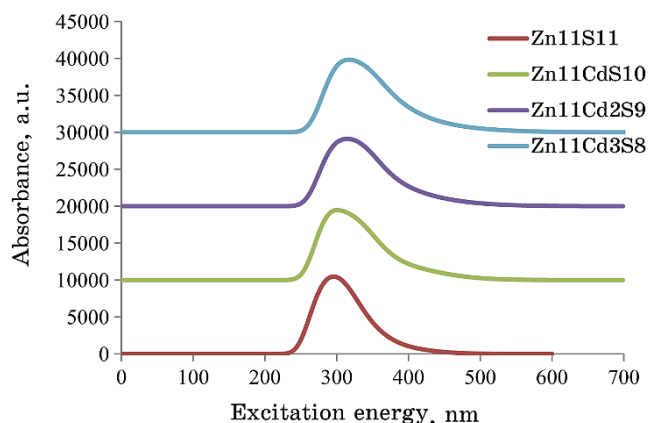


**Fig. 6.** UV−Vis spectra for nanostructures.

mental longitudinal optical mode (LO mode) value of 250 $cm^{-1}$ [18]. The quantum confinement effect was produced, shifting in the frequency of 6 $cm^{-1}$.

Changing the zinc atoms by cadmium atoms caused shifting and widening in maximum peak, also new peaks have appeared, this indicating construct the ternary alloys from zinc, sulphide, and cadmium atoms as shown in Table 2.

### 3.4. UV−Visible Spectra

Electrons can jump from high occupied molecular orbital (HOMO) to lower unoccupied molecular orbital (LUMO) by stimulating energy from ultraviolet and visible light. At the nanoscale regime, the confinement effect and surface to volume ratio produced increasing in the energy level separation and widening in the energy gap compared with bulk. Therefore, the ternary alloy nanostructure has optoelectronic properties dependent on size, shape or phase, and composition.

Figure 6 shows the UV−Vis spectra of the ternary alloys nanostructures. As seen from Figure 6, the UV−Vis spectrum for

**TABLE 3.** Maximum peaks for the UV−Vis spectra.

| Nanostructures | UV−Vis ($\lambda_{max}$), nm |
|---|---|
| $Zn_{11}S_{11}$ | 295.2 |
| $Zn_{10}CdS_{11}$ | 301 |
| $Zn_9Cd_2S_{11}$ | 315 |
| $Zn_8Cd_3S_{11}$ | 316.8 |

$Zn_{11}S_{11}$ has a maximum peak at 295.2 nm (4.2 eV), which is corresponding to the ZnS experimental value of 3.6 eV [14, 19], the replacement of zinc atoms by cadmium atoms caused decreasing in energy levels.

Thus, the maximum peaks shifted to lower energy as shown in Table 3. Also from Fig. 6, the optical edge absorption shift to lower energy and the width of peaks increased with increased cadmium atoms.

## 4. CONCLUSIONS

Representing the cubic structure by tetramantane molecule for zinc sulphide and ternary alloys constitute from zinc, cadmium, and sulphide $Zn_{11}Cd_nS_{11}$ ($n = 1-3$) gave results with good agreement with practical measurement. Increasing the concentrations of cadmium atoms produced contracted in LUMO−HOMO gap, and it became of 3.088244 eV for $Zn_{11}Cd_3S_8$. IR and Raman spectra for $Zn_{11}Cd_nS_{11}$ ($n = 1-3$) referred to appear new peaks different from $Zn_{11}S_{11}$. This indicated to construct the ternary alloys from zinc, cadmium, and sulphide atoms. The maximum peaks and the optical absorption edge for UV−Vis spectra of $Zn_{11-n}Cd_nS_{11}$ ($n = 1-3$) shift to lower energy with increased concentrations of cadmium atoms. Regulating the value of maximum peaks and the optical absorption edge by varying the composition of alloy attends in several applications such as optoelectronic devices and biosensors.

## REFERENCES

1. P. I. Gouma, *Pan Stanford Publishing* (Pte. Ltd: 2010), p. 4.
2. E. Sanville, A. Burnin, and J. J. Belbruno, *J. Phys. Chem A*, **110**, No. 7: 2378 (2006).
3. X. Wang, Z. Xie, H. Huang, Z. Liu, D. Chen, and G. Shen, *J. Mater. Chem.*, **22**: 6845 (2012).
4. D. Maske, *International Journal of Scientific and Research Publications*, **6**, No. 6: 264 (2016).
5. C. S. Yang, Y. P. Hsieh, M. C. Kuo, P. Y. Tseng, Z. W. Yeh, K. C. Chiu,

J. L. Shen, A. H. M. Chu, W. C. Chou, and W. H. Lan, *Materials Chemistry and Physics*, **78**: 602 (2003).

6. M. A. Abdulsattar, *Carbon Lett.*, **16**: 192 (2015).

7. M. A. Abdulsattar and I. S. Mohammed, *Comput. Mater. Sci.*, **91**: 11 (2014).

8. M. A. Abdulsattar, H. M. Abduljalil, and H. H. Abed, *Karbala International Journal of Modern Science*, **5**: 119 (2019).

9. M. A. Abdulsattar, H. M. Abduljalil, and H. H. Abed, *Calphad*, **64**: 37 (2019).

10. B. B. Kadhim, M. A. Abdulsattar, and A. M. Ali, *International Journal of Modern Physics B*, **33**, No. 16: (2019).

11. E. Sanville, A. Burnin, and J. J. Bel Bruno, *J. Phys. Chem. A*, **110**: 2378 (2006).

12. M. J. Frisch, G. W. Trucks, H. B. Schlegel, G. E. Scuseria, M. A. Robb, J. R. Cheeseman, G. Scalmani, V. Barone, B. Mennucci, G. A. Petersson, H. Nakatsuji, M. Caricato, X. Li, H. P. Hratchian, A. F. Izmaylov, J. Bloino, G. Zheng, J. L. Sonnenberg, M. Hada, M. Ehara, K. Toyota, R. Fukuda, J. Hasegawa, M. Ishida, T. Nakajima, Y. Honda, O. Kitao, H. Nakai, T. Vreven, J. A. Montgomery, Jr, J. E. Peralta, F. Ogliaro, M. Bearpark, J. J. Heyd, E. Brothers, K. N. Kudin, V. N. Staroverov, R. Kobayashi, J. Normand, K. Raghavachari, A. Rendell, J. C. Burant, S. S. Iyengar, J. Tomasi, M. Cossi, N. Rega, J. M. Millam, M. Klene, J. E. Knox, J. B. Cross, V. Bakken, C. Adamo, J. Jaramillo, R. Gomperts, R. E. Stratmann, O. Yazyev, A. J. Austin, R. Cammi, C. Pomelli, J. W. Ochterski, R. L. Martin, K. Morokuma, V. G. Zakrzewski, G. A. Voth, P. Salvador, J. J. Dannenberg, S. Dapprich, A. D. Daniels, O. Farkas, J. B. Foresman, J. V. Ortiz, J. Cioslowski, and D. J. Fox, *Gaussian 09. Revision E.01* (Wallingford CT Inc.: 2009).

13. *Handbook of Magnetic Materials* (Ed. K. H. J. Buschow) (Elsevier Science: 2006), vol. **16**.

14. K. Hedayati, A. Zendehnam, and F. Hassanpour, *Journal of Nanostructures*, **6**, No. 3: 207 (2016).

15. G. N. Chaudhari, S. Manorama, and V.J. Rao, *Thin Solid Films*, **208**: 243 (1992).

16. Y. Yesu Thangam, R. Anitha, and B. Kavitha, *Journal of Applied Sciences and Engineering Research*, **1**, No. 2: 282 (2012).

17. G. G. Hammes, *Spectroscopy for the Biological Sciences* (Hoboken, New Jersey: Wiley: 2005).

18. P. Kumar, J. Singh, M. K. Pandey, C. E. Jeyanthi, R. Siddheswaran, M. Paulraj, N. Hui, and K. S. Hui, *Materials Research Bulletin*, **49**: 144 (2014).

19. A. L. Stroyuk, A. E. Raevskaya, A. V. Korzhak, and S. Y. Kuchmii, *Journal of Nanoparticle Research*, **9**: 1027 (2007).